

Analysis of a Dynamic Maximum Power Point Tracker for Photovoltaic Applications

Stephen Moore
Andy Welch

ABSTRACT

To efficiently operate photovoltaic cells for electric power generation a maximum power tracker circuit is required. Photovoltaic cells exhibit behavior in which there is one unique operating point that yields the highest power output. The operating point changes with varying degrees of solar insolation and thus a device is required to constantly make adjustments to maintain peak power. Traditional approaches of peak power tracking have classically relied on the slow and fundamentally sub-optimal perturbation technique. The object of this paper is to verify the operation of a control algorithm that uses the input current and voltage ripple resulting from the boost converter circuitry as a dynamic perturbation. This method eliminates the need for external perturbation and increases response time. The photovoltaic cell and the boost converter are modeled, and a control algorithm is presented and verified.

INTRODUCTION

The environmental conditions in which photovoltaic cells are employed for power generation purposes are usually highly susceptible to seasonal and weather effects. Photovoltaics operate at peak efficiency only at one unique operating point, and any changes in insolation due to cloud conditions, time of day, and season will result in sub-optimal operation. A maximum peak power tracker (MPPT) is introduced that employs a control strategy that converges on the optimal operating point rapidly when exposed to changing solar conditions. Photovoltaic cell for electricity generation are usually large and expensive thus an efficient MPPT is required to maximize the economic benefits of solar power.

The MPPT algorithm presented in this paper is a rapidly converging, highly efficient converter due to the nature of the control algorithm. Traditional approaches usually rely on perturbation of the operating point to confirm optimal operation. This method presented does not rely on any artificially introduced perturbation but uses the switching ripple of a boost converter to serve as the perturbation.

The photovoltaic cell's parameters are identified and modeled. The boost dc/dc converter is introduced and the photovoltaic characteristic equations are used to derive the boost converter governing equations. Several approximations are made to construct the governing equations and rational is presented for each step. The final system is simulated using the developed control algorithm.

PHOTOVOLTAIC PARAMETERS AND CHARACTERIZATION

An illuminated photovoltaic cell configured for power generation will operate in the first quadrant region, with both the current through the cell and the voltage across the cell staying positive. For power tracking application only the first quadrant region needs to be examined. For a power generating illuminated photovoltaic cell, the governing equation for current and voltage is

$$V = \frac{A \cdot k \cdot T}{q} \cdot \ln \left(\frac{I_{ph} - (1 + R_{sh} \parallel R_s) \cdot I - \frac{V}{R_{sh}} + I_o}{I_o} \right) - R_s \cdot I$$

where V and I are cell terminal voltage and current, I_{ph} is the photocurrent, I_o is the diode reverse saturation current, R_s is series resistance, R_{sh} is shunt resistance, and T is absolute temperature. The first term of the equation contains constants, where A is the completion factor, k is Boltzmann's constant, and q is the electron charge. Substituting $\beta = 1 + R_{sh} \parallel R_s$ and $\Lambda = q/AkT$, the equation becomes

$$V = \frac{1}{\Lambda} \cdot \ln \left(\frac{I_{ph} - \beta \cdot I - \frac{V}{R_{sh}} + I_o}{I_o} \right) - R_s \cdot I$$

The photovoltaic cell presented represents a typical solar cell with: $\Lambda = 13.7 \text{ } ^1/V$, $I_{ph} = 0.8 \text{ A}$ (at solar insolation of 1000 W/m^2 , $I_o = 0.5 \text{ mA}$, $R_s = 0.05 \text{ } \Omega$, $R_{sh} = 10^5 \text{ } \Omega$. It is also known that solar cell voltage is reduced by $-0.4\%/^{\circ}\text{C}$.

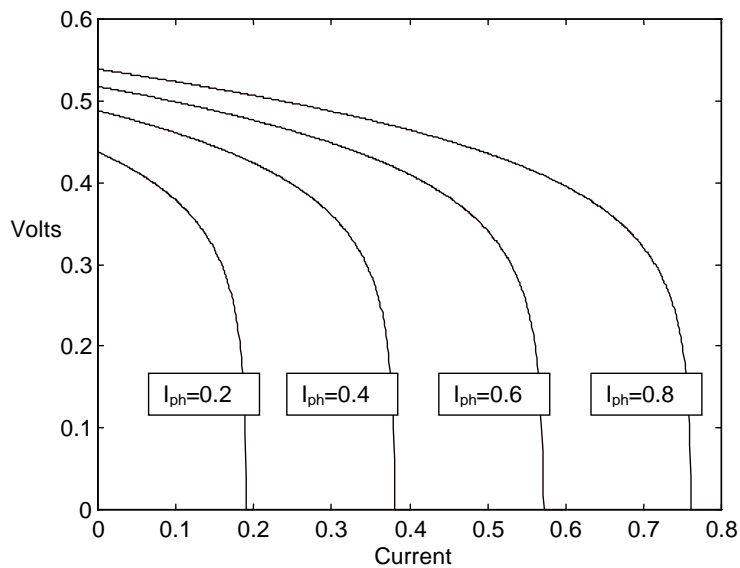


Figure 1 Solar Cell Volt-Ampere Characteristics for Different Solar Insolation Levels

From Fig.1 it can be seen that the photovoltaic has a different volt-ampere curve for different values of solar insolation levels (reflected in photocurrent I_{ph}). For each value of I_{ph} , there are two unique points that define the scaling of the volt-ampere curve: V_{OC} is defined as the open circuit voltage of the cell and is a global maximum that occurs when the cell current is zero. I_{SC} is defined as the short circuit current of the cell and is a global maximum when the cell voltage is zero. Between these two points there is a unique point in which the product of V and I is maximum. This point is called the maximum power point of the volt-ampere curve at photocurrent level I_{ph} and is usually located where the voltage is non-linearly decreasing rapidly. Refer to Figure 2 for the I-V curve and its corresponding peak power point.

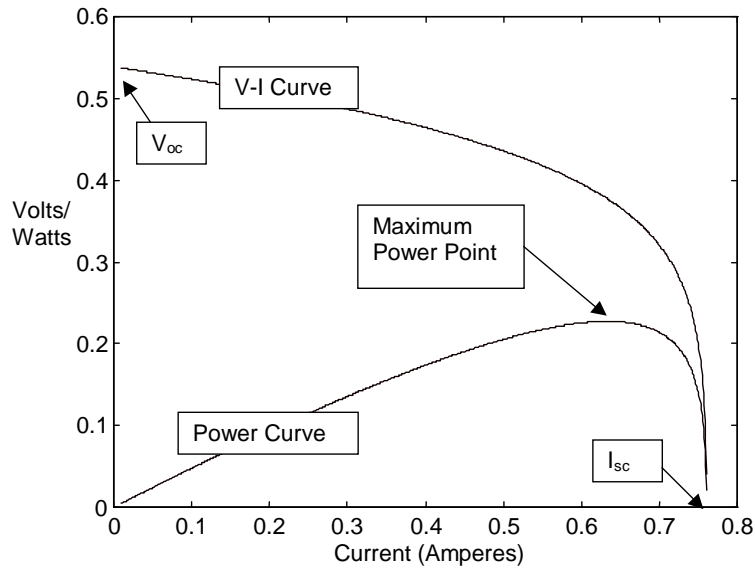


Figure 2 Solar Cell V-I Curve and Power Curve for $I_{ph}=0.8$

Solving Eq.(1) for $V(I)$ does not give a closed form solution due to the term V/R_{sh} located in the natural logarithm. Considering that the voltage at the maximum power point typically operates above 0.3 Volts, the term V/R_{sh} is 10^5 smaller than the βI term, thus can be neglected in this study. Figure 2 illustrates the difference between Eq.(1) with and without the V/R_{sh} term at various solar insolation levels.

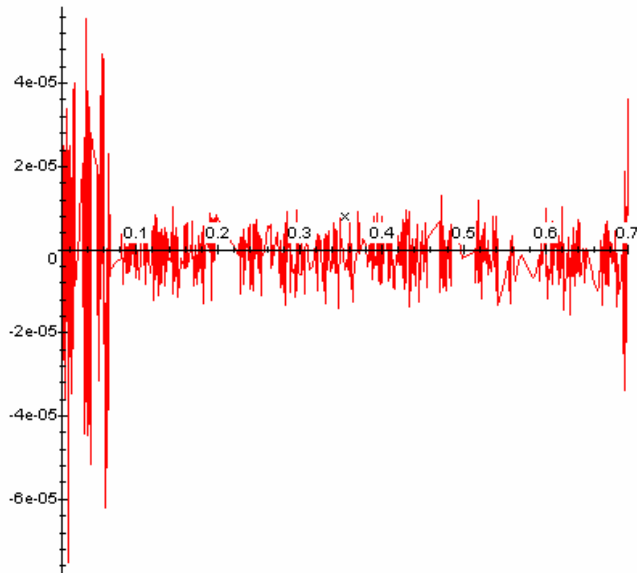


Figure 2 Difference Between Equations () and ()

After the substitutions and simplification, Eq.(1) becomes:

$$V = \frac{1}{\Lambda} \cdot \ln\left(\frac{I_{ph} - \beta \cdot I + I_o}{I_o}\right) - R_s \cdot I$$

The value for V_{OC} is easily computed by substituting in a zero value for I in Eq.(3). Solving this equation V_{OC} ,

$$V_{oc} = \frac{1}{\Lambda} \cdot \ln\left(\frac{I_{ph} + I_o}{I_o}\right)$$

The value for I_{SC} is somewhat more difficult to compute because of the nonlinear term inside the natural logarithm. However, because the value $R_s I$ is significantly smaller it can be neglected to compute I_{SC} as approximately

$$I_{sc} = \frac{I_{ph}}{\beta}$$

BOOST CONVERTER TOPOLOGY

The design constraints allowed for the adaptation of a simplified boost converter topology (see Figure 3). As the peak power control algorithm is based on photovoltaic current and voltage ripple caused by the switching transistor, no input filter capacitor was required. Because the battery is in essence a stiff voltage source capable of absorbing infinite current, no output filter capacitor was required. Thus the boost converter topology is reduced a single inductor, first order system. The solar cell is modeled on the schematic as a current controlled voltage source using Eq.(3) as the transfer function. The boost converter needs to be configured for continuous conduction for optimal performance because any discontinuity would mean periods in which the available power from the solar cell was not being fully utilized (Figure 4).

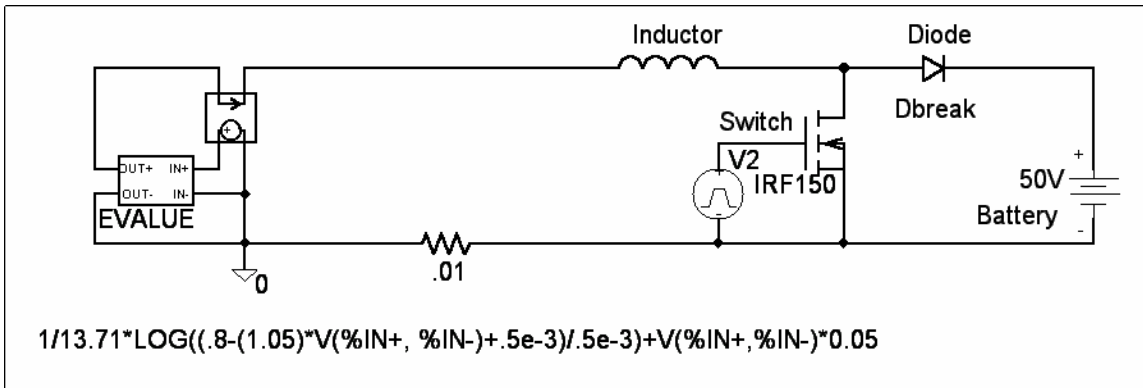


Figure 3 Simplified Boost Converter Topology

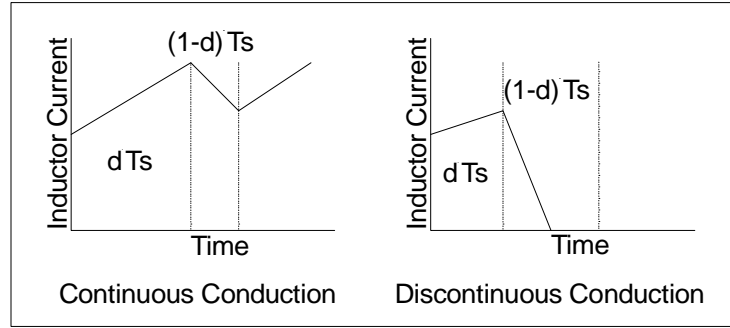


Figure 4 Continuous vs. Discontinuous Conduction

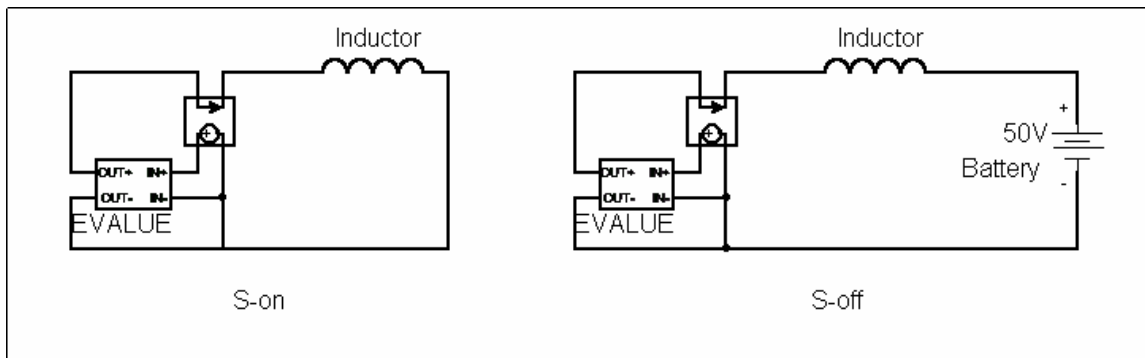


Figure 5 Boost Converter Continuous Conduction States

The boost converter operating in continuous conduction has two states (Figure 5). During the S-on state, the transistor is turned fully on. The inductor current i is increasing due to the current output of the photovoltaic and no output current flows to the battery. The differential equation governing the S-on period is:

$$L \frac{di}{dt} = v_s(i)$$

Substituting Eq.(3) for v_s ,

$$\frac{di}{dt} = \frac{1}{L} \left(\frac{1}{\Lambda} \cdot \ln \left(\frac{I_{ph} - \beta \cdot i + I_o}{I_o} \right) - R_{sh} \cdot i \right)$$

The governing equation for the S-off period is:

$$L \frac{di}{dt} + v_s(i) = V_b$$

Substituting Eq.(3) for v_s ,

$$\frac{di}{dt} = \frac{1}{L} \left(V_b - \frac{1}{\Lambda} \cdot \ln \left(\frac{I_{ph} - \beta \cdot i + I_o}{I_o} \right) + R_{sh} \cdot i \right)$$

Equations (7) and (9) are nonlinear differential equations that cannot be solved directly. The βi term in the numerator of the logarithm function forces the use of a Lambert ('W') function to be employed for an exact solution. A Lambert function is described as a function in that

$$\text{LambertW}(x) \cdot e^{\text{LambertW}(x)} = x$$

The Lambert function has an infinite number of solution 'branches,' with exactly one principle branch analytic at zero. This function is exceedingly difficult to do by hand and a computer simulation is required to solve for the solutions. A series approach was then employed to solve the differential equations. A third order series solution for Eq.(9) is

$$i(t) = i(0) - \frac{V_b \cdot \Lambda - \ln\left(\frac{I_{ph} - \beta \cdot i(0) + I_o}{I_o}\right) + i(0) \cdot R_s \cdot \Lambda}{L \cdot \Lambda} + \frac{1}{2} \frac{\left(V_b \cdot \Lambda - \ln\left(\frac{I_{ph} - \beta \cdot i(0) + I_o}{I_o}\right) + i(0) \cdot R_s \cdot \Lambda\right) \cdot (\beta + R_s \cdot \Lambda \cdot I_{ph} - R_s \cdot \Lambda \cdot \beta \cdot i(0) + R_s \cdot \Lambda \cdot I_o)}{L^2 \cdot \Lambda^2 \cdot (I_{ph} - \beta \cdot i(0) + I_o)}$$

The solution for Eq.(7) was computed similarly. A computer simulation of the exact solution was used for comparison purposes to validate the third order series approximation Equation (11). The result of the analysis is presented in Figure 6. The error does not exceed 1E-5 so the third order series approximation is valid for this analysis.

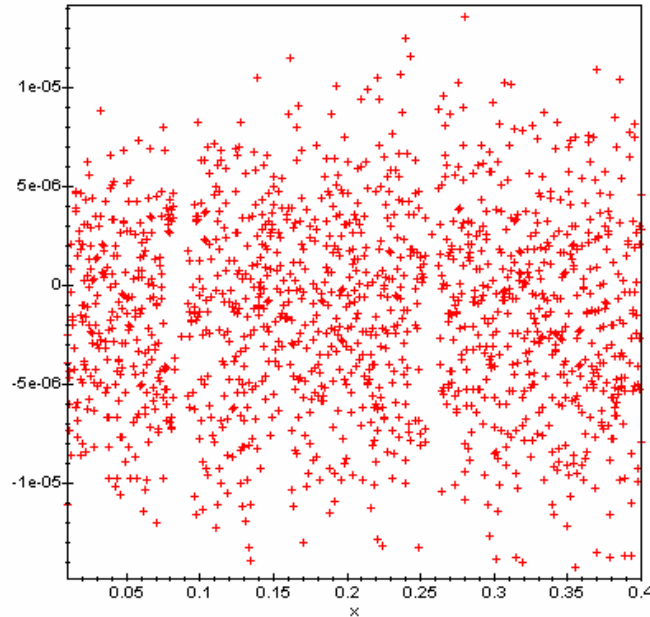


Figure 6 Error Between the Exact Solution and Third Order Series Approximation for Eq.(9)

CONTROL ALGORITHM

The perturbation technique has been commonly employed as the traditional approach to maximum power point tracking. Using this technique, the control algorithm will sense the output

current and voltage to measure power. Then a known perturbation is added to the control signal and power is again sensed at the end of the perturbation, hence determining which direction to shift the operating point to reduce the differential to zero. This classical method is fundamentally sub-optimal and requires long time scales for the control to find the maximum power point. A useful variation of this strategy is to only measure battery current to compute power with. Because the battery voltage is 'stiff' and does not change between cycles, any change in current can be directly interpreted as a change in power. This method still requires perturbation to operate, albeit with a reduced amount of circuitry.

The object of this paper is to verify the operation of a control algorithm that uses the input current and voltage ripple resulting from the boost converter circuitry as a dynamic perturbation. The boost converter switching transistor presents a constantly changing load to the photovoltaic source, resulting in switching ripple in the input current and voltage. The ripple itself can be measured and used to obtain an optimal switching duty cycle to operate on the maximum power point. This type of measurement techniques allows the control circuitry to converge orders of magnitude faster than traditional approaches.

The boost converter can operate in four different modes that the control circuitry must track the maximum power point in. Refer to Figure 7 for the four operating modes.

1. dp/dt increasing when di/dt positive and dv/dt negative.
2. dp/dt decreasing when di/dt negative and dv/dt positive.
3. dp/dt decreasing when di/dt positive and dv/dt negative.
4. dp/dt increasing when di/dt negative and dv/dt positive.

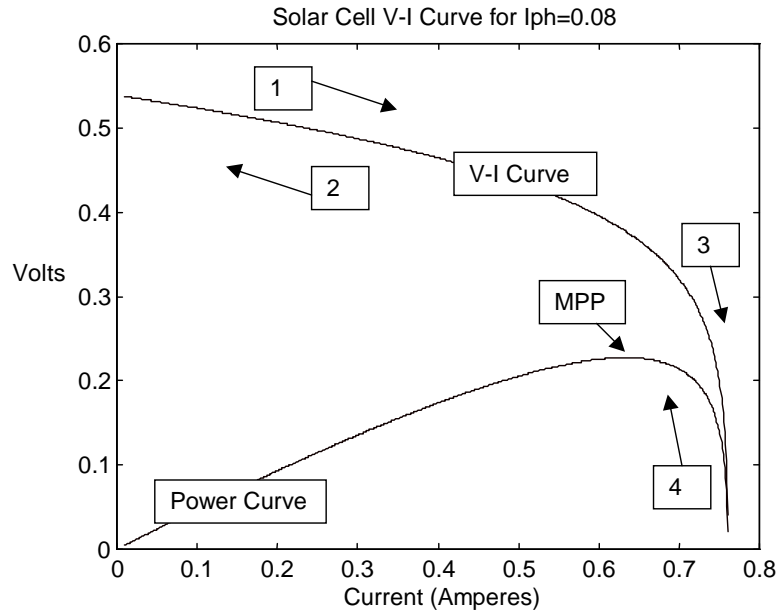


Figure 7 Four Modes of Control Operation

For each of the four modes of operation, dp/di and dp/dv can be computed. For modes in which current is too low (modes 1 and 2), dp/dv will be positive and dp/di negative. In modes in which current is too high (modes 3 and 4), dp/dv will be negative and dp/di positive. It is important to point out that the quantity dp/dv can be computed from the chain rule:

$$\frac{\partial p}{\partial v} = \frac{dp}{dt} \cdot \frac{dv}{dt}$$

and similarly for dp/di . The control strategy uses the value dp/dv to track the maximum power point. The quantity di/dp could be used in the same manner. However, because the voltage

slope is much steeper than the current slope on the V-I curve at the maximum power point, dp/dv is more sensitive than dp/di . Using the chain rule rate of change of power can be found by

$$\frac{dp}{dt} \cdot \frac{dv}{dt} = \left(i \cdot \frac{dv}{dt} + v \cdot \frac{di}{dt} \right) \cdot \frac{dv}{dt}$$

Integrating dp/dv over a single switching cycle in respect to time indicates the power tracker operation's net deviation from the maximum power point. A negative value for dp/dv indicates that the current is too high for maximum power, and a positive value indicates insufficient current:

$$\int \frac{dp}{dt} \cdot \frac{dv}{dt} dt = \int \left(\frac{dv}{dt} \right)^2 \frac{dp}{dv} dt$$

A change in duty cycle can now be computed by taking the derivative of Eq.(x):

$$\Delta d = -k \cdot \left(\frac{dv}{dt} \right)^2 \frac{dp}{dv}$$

where Δd is the change in duty cycle and k is a gain constant. The constant k scales Δd to match the size of the photovoltaic system. For the single cell model with $I_{ph} = 0.8$ Amperes, the k used was $1E-7$ to correspond to the di of the system. Use of a larger k would result in a Δd overshoot and would result in oscillations. The negative multiplier to force the duty cycle up (higher boost) when current is lower than the maximum power point, and vice-versa.

This type of peak power tracking can only be employed for power sources with no local maxima on either the current or voltage characteristics. Photovoltaic cells display characteristics with unique global maximas at V_{OC} and for I_{SC}

MODEL RESULTS

A computer simulation was constructed to evaluate the performance of the control algorithm. The simulation was executed using the Matlab software package. Because all of the governing equations have closed form solutions, the simulation did not have to solve any differential or simultaneous equations. A simplified block diagram of the system structure is illustrated below in Figure 8:

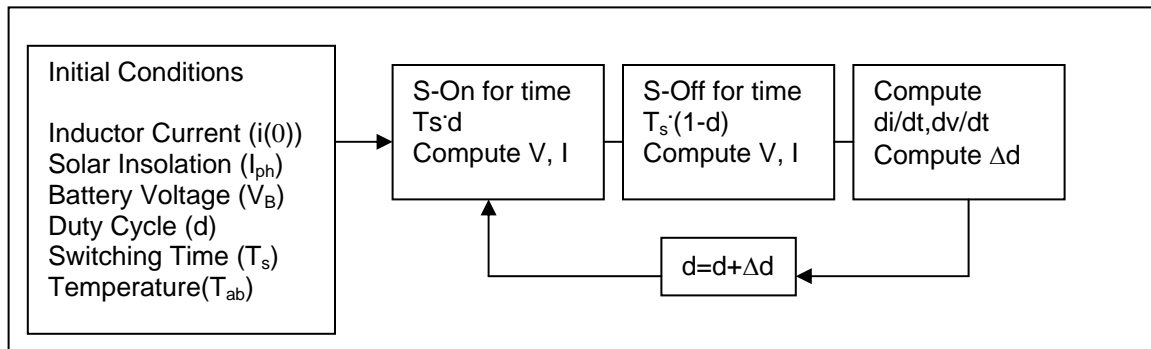


Figure 8 Block Diagram of System Simulation

The simulation incorporated the constants for the typical solar cell previously specified with Eq.(2). Temperature was held at a constant standard operating condition, however, the voltage computation includes a $-0.4\%/^{\circ}\text{C}$ compensation term for future analysis. A solar cell will normally have high fluctuations in temperature because a typical solar cell is about 15% efficient, which leaves 85% of incoming solar radiation to be either reflected or absorbed by the cell in the form of heat.

The simulation was run at a constant solar insolation $I_{ph} = 0.8$ level starting at an initial duty cycle of 95% and zero initial inductor current. The control algorithm requires start-up at a high duty cycle to avoid discontinuous conduction. A 2 volt battery was used as the load. Figure 9 shows the results of the control algorithm run for 350 switching cycles with zero initial current in the inductor. Notice that the duty cycle converges rapidly (<50 switching cycles).

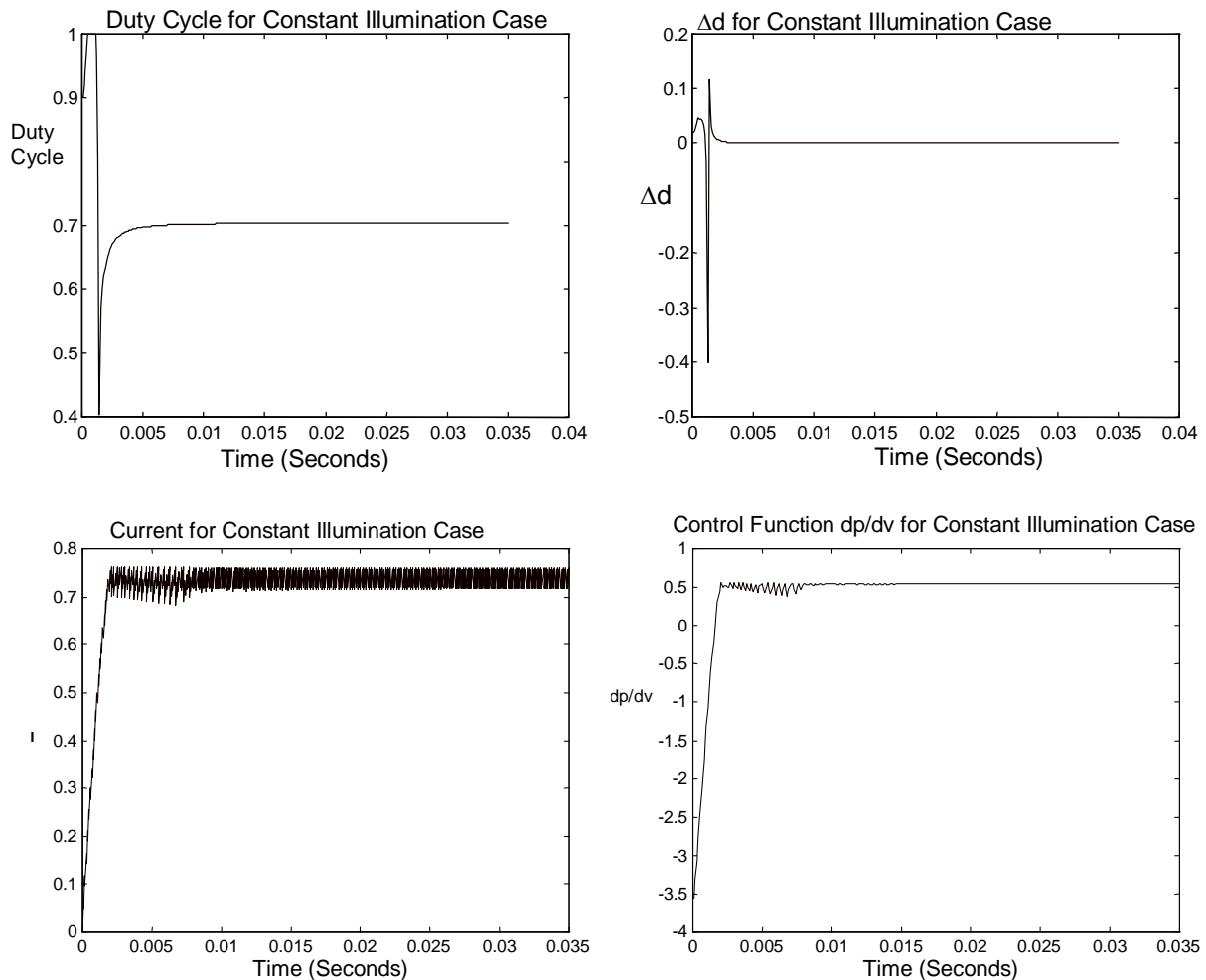


Figure 9 Duty Cycle Convergence for Constant $I_{ph} = 0.8$ Case

A step change of was inserted into the control algorithm to simulate an increase of insolation by $I_{ph} = 0.7$ to $I_{ph} = 0.8$ after 150 switching cycles. The results of this simulation are presented as Figure 10. Notice that the control initially converged to the maximum power point within 50 switching cycles and compensated for the increased insolation within about the same amount of time. An interesting side note is to consider adding a small filter capacitor across the photovoltaic cell's output. The switching current causes the photovoltaic voltage to fluctuate considerably, as reflected in the Power Graph of Figure 9. This fluctuation is what allows the control algorithm to converge efficiently so it can not be filtered out. However, a filter capacitor

can be chosen to reduce the voltage ripple down an order of magnitude. Notice that on Figure 10 that the power fluctuates significantly more with $I_{ph} = 0.7$ than at the higher I_{ph} , thus a proper filter capacitor would increase power output in low lighting conditions while retaining control capability.

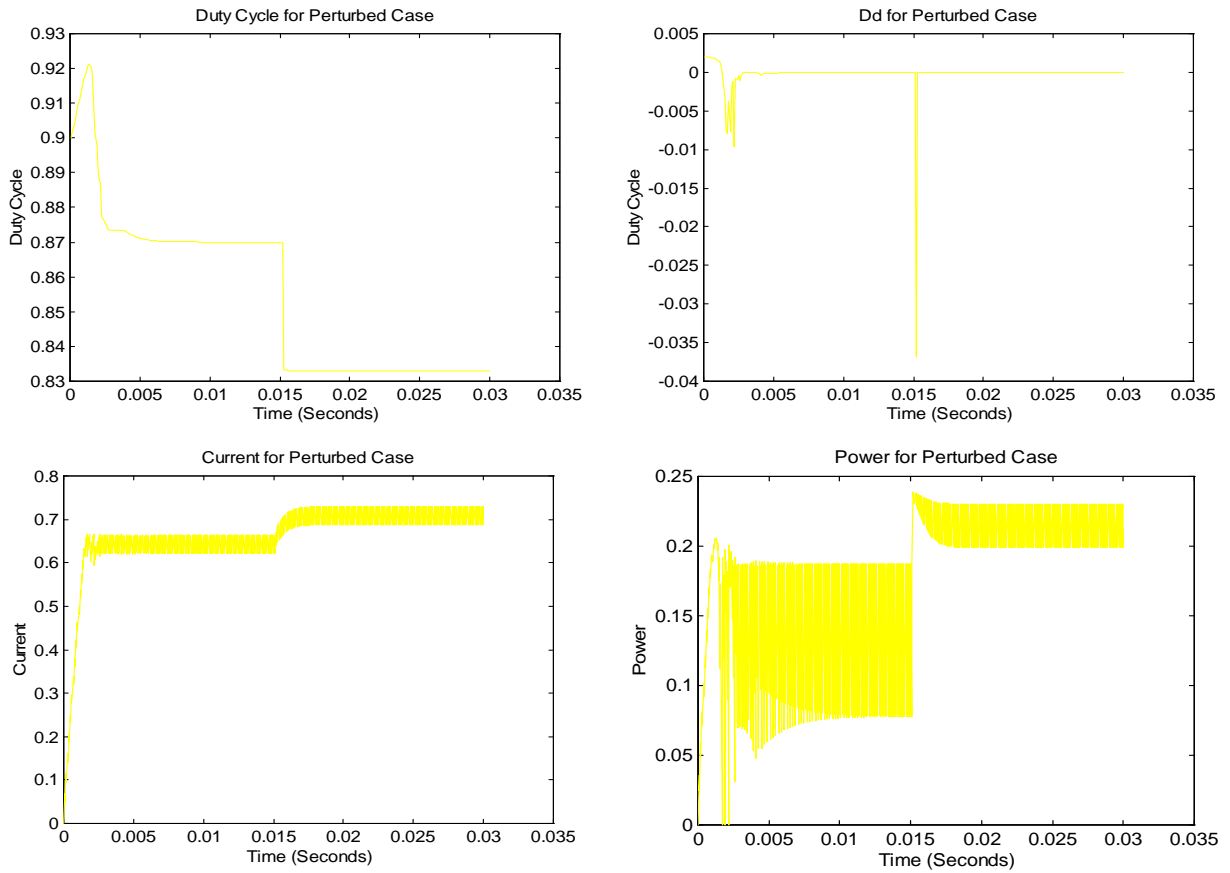


Figure 10 Perturbed Case System Performance

Figure 10 illustrates how the MPPT oscillates up and down the $I_{ph} = 0.7$ V-I curve to find the maximum power point then moves to the $I_{ph} = 0.8$ curve. Also illustrated is the power curve.

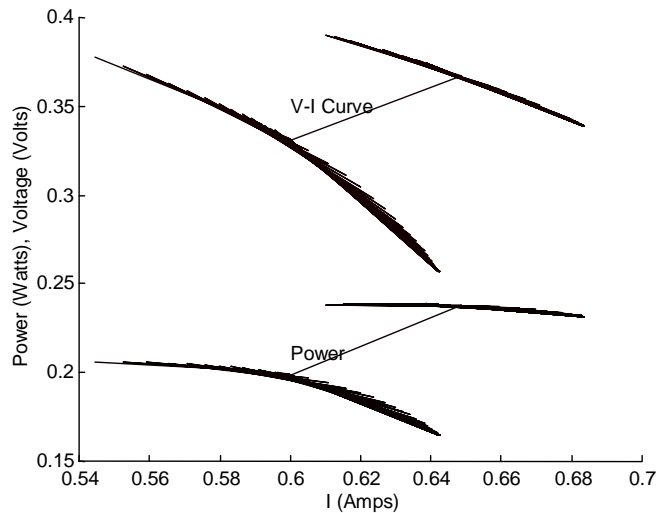


Figure 11 Maximum Power Tracking for Perturbed Case